DYNAMIC RESPONSE EVALUATION ON CURVED TWIN I-GIRDER BRIDGE USING VEHICLE-BRIDGE COUPLED VIBRATION ANALYSIS

X. HE[1*], T. SHIMODA[2†], T. HAYASHIKAWA[1], M. KAWATANI[3], and T. MATSUMOTO[1]

[1]*Faculty of Engineering, Hokkaido University, Japan*
[2]*Graduate School of Engineering, Hokkaido University, Japan*
[3]*Graduate School of Engineering, Kobe University, Japan*

ABSTRACT

This study is intended to evaluate the dynamic response of the curved twin I-girder bridges, using a developed numerical approach that can simulate the coupled vibration of the bridge and running vehicles. A typical curved twin I-girder bridge modeled with three-dimensional beam elements is used for the analyses. A general large dump truck is modeled as a sprung-mass dynamic system with 12 degree-of-freedoms. The coupled vibration of the interaction system is formulized, based on which a computer program is developed. To investigate the basic dynamic characteristics of the curved bridges, eigenvalue analyses of different type bridges are carried out. Then, the dynamic responses of the bridge are evaluated considering different running conditions of the vehicles.

Keywords: Curved bridge, Vehicle-bridge interaction, Dynamic response analysis, Torsional stiffness

1. INTRODUCTION

Owing to the rising cost reduction demands in Japan, rationalized girder bridges such as twin I-girder bridges have been gradually put into practical use, which is expected to be more economical and easy to maintain (Yoon et al. 2005). This type of bridge was designed and constructed in France in early 1960s and in Japan in 1990s (kim et al. 2004). However, the low torsional stiffness of the rationalized girder bridge is concerned, especially for curved ones (Linzell et al. 2004). Therefore, the dynamic characteristics of such bridges should be fully investigated to ensure their structural safety. On the other hand, the traffic induced-vibration problems due to the recently growing traffic loads are also important issues. The low torsional stiffness may lead to excessive vibration that can cause structural fatigue or environmental vibration problems, etc. In order to discuss such problems, it is necessary to theoretically clarify the phenomena at first.

The purpose of this study is to evaluate the dynamic response of the curved twin I-girder bridges, using a developed numerical approach that can simulate the coupled vibration of the bridge and running vehicles. In this paper, a curved twin I-girder bridge with general cross-section is adopted

* Corresponding author: Email: xingwen_he@eng.hokudai.ac.jp

† Presenter: Email: mei29735@yahoo.co.jp

for the analysis. A general large dump truck with one axis at front and two axes at rear is modeled as a sprung-mass dynamic system with 12 degree-of-freedoms (DOFs). The coupled vibration of the interaction system is formulized and a computer program is developed. To investigate the basic characteristics of the curved twin I-girder bridges and to find acceptable torsional stiffness of the superstructure, eigenvalue analyses of two different type bridges are carried out and compared with each other. Then, the coupled vibrations of the running vehicle and the two types of bridges are simulated to evaluate the dynamic response of the curved girder bridge under critical vehicle running conditions, in which the influence of resonant excitation caused by the wheel distance and the speed of running vehicles on the dynamic response of the bridge is elucidated.

2. TWIN I-GIRDER BRIDGE MODELS

In this study, a curved twin I-girder bridge with general cross-section as shown in Figure 1 is adopted, which has a span length of 50 m. This bridge has a PC slab with 0.3 m thickness. The middle crossbeams with I-shaped cross-section are perpendicularly connected to the centers of the main girders in vertical direction, while the end ones are connected at the upper sides of the girders. The crossbeams are aligned along the main girders in longitudinal direction at an interval of 5 meter. The material properties of the PC slab and steel members are shown in Table 1. The dimensions of I-shaped beam cross-sections used in this analysis are given in Table 2. The boundary condition of this bridge is simply-support, in which the movable pin bearings are free in x-direction.

The three-dimensional beam element model of the twin I-girder bridge superstructure is shown in Figure 2 and designated as the basic model. The main girders and crossbeams are modeled as beam elements along their centroids. The PC slab is also modeled with beam elements, which are converted from the slab plates considering equivalent mass and stiffness. The girder beam elements and those of the slab are connected with offset members in the vertical direction.

To increase the torsional stiffness, a countermeasure is devised as shown in Figure 3, changing the perpendicular I-shaped crossbeams into diagonal ones with same properties. The eigenvalue analyses of these two models are carried out to evaluate their difference of the torsional stiffness. The curvature radii of both bridge models are the same as R=200m.

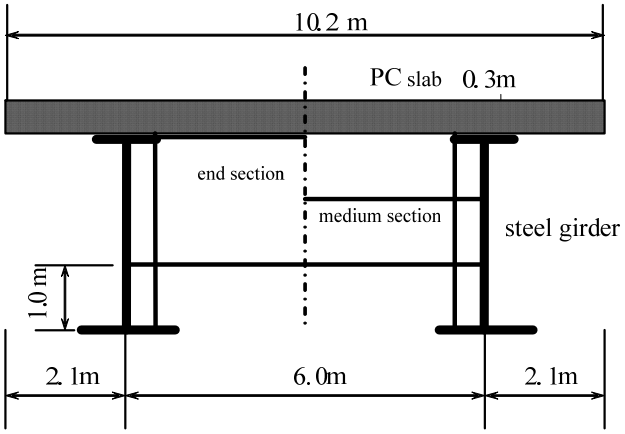

Figure 1: Cross-section of twin I-girder bridge

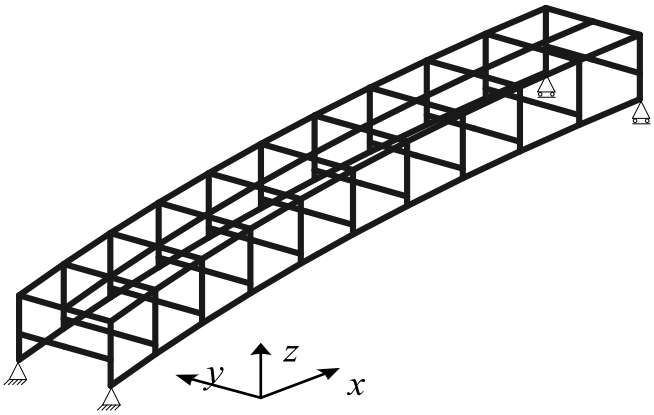

Figure 2: Basic model

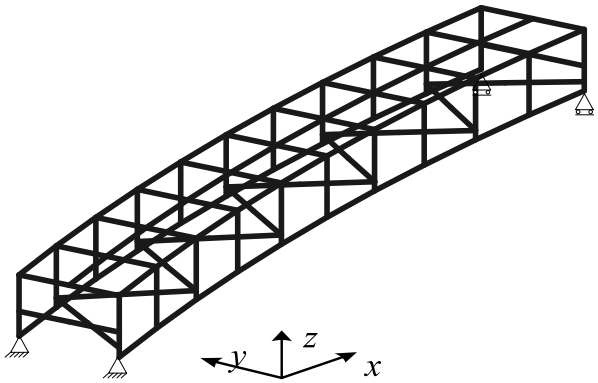

Figure 3: Diagonal reinforcement model

Table 1: Properties of bridge members

	PC slab	Steel member
Young's modulus E (N/mm^2)	2.857×10^4	2.000×10^5
Poisson's ratio μ	0.2	0.3
Unit weight w (kN/m^3)	24.5	77.0

Table 2: Cross-section properties of bridge steel members

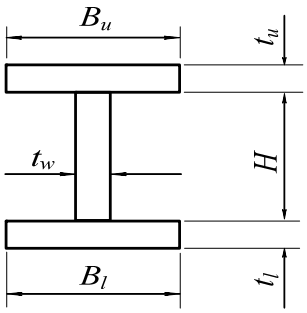

Unit (mm)

	Main girder	End crossbeam	Middle crossbeam
B_u	500	300	300
T_u	30	25	25
H	3000	2000	1000
t_w	24	16	16
B_l	800	300	300
t_l	50	25	25

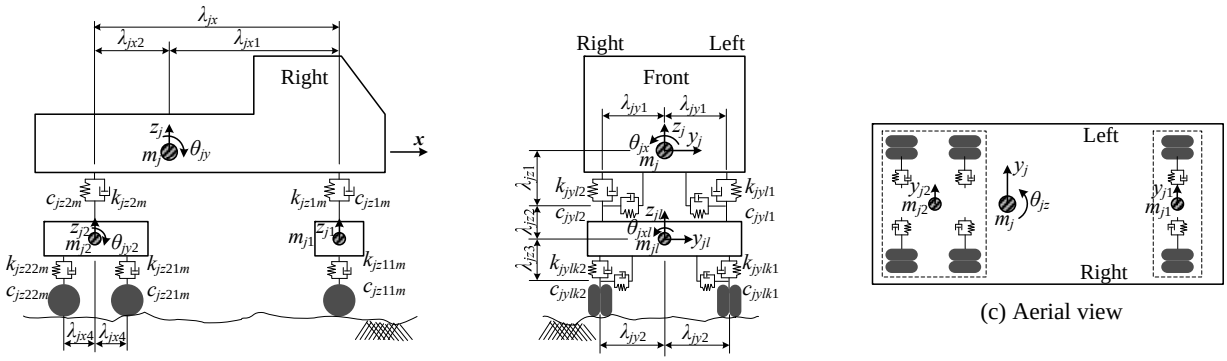

(a) Side view (b) Front view (c) Aerial view

Figure 4: 12-DOF vehicle model

Table 3 (a): Variants used for the 12-DOF vehicle model

Division	Definition	Notation
Parameter	Sprung mass including payload	m_j
	Unsprung masses	m_{jl}
	Moment of inertia of sprung mass	I_{jx}, I_{jy}, I_{jz}
	Moment of inertia of unsprung masses	I_{jxl}, I_{jyl}
	Spring constant of suspensions	k_{jylm}, k_{jzlm}
	Spring constant of tires	k_{jylkm}, k_{jzlkm}
	Damping coefficient of suspensions	c_{jylm}, c_{jzlm}
	Damping coefficient of tires	c_{jylkm}, c_{jzlkm}
Geometry	Distance between front and rear axles	λ_{jx}
	Distance between axles and body centroid	λ_{jxl}
	1/2 distance of tandem axles	λ_{jx4}
	1/2 distance between upper vertical springs in *y*-direction	λ_{jy1}
	1/2 tread	λ_{jy2}
	Distance from body centroid to upper horizontal springs	λ_{jz1}
	Distance from suspension centroid to upper horizontal springs	λ_{jz2}
	Distance from suspension centroid to lower horizontal springs	λ_{jz3}

Table 3 (b): Degree-of-freedoms of the vehicle model

Definition	Notation
Sway of the sprung mass (body)	y_j
Bouncing of the sprung mass (body)	z_j
Rolling of the sprung mass (body)	θ_{jx}
Pitching of the sprung mass (body)	θ_{jy}
Yawing of the sprung mass (body)	θ_{jz}
Sway of the front unsprung mass	y_{j1}
Parallel hop of the front unsprung mass	z_{j1}
Axle tramp of the front unsprung mass	θ_{jx1}
Sway of the rear unsprung mass	y_{j2}
Parallel hop of the rear unsprung mass	z_{j2}
Axle tramp of the rear unsprung mass	θ_{jx2}
Windup of the rear unsprung mass	θ_{jy2}

3. COUPLED VIBRATION ANALYSIS OF VEHICLE-BRIDGE SYSTEM

3.1 Vehicle-bridge interaction analysis procedure

In this paper, dynamic responses of the vehicle-bridge interaction system are simulated using a developed computer program based on the formulization process described below. Modal analysis technique is applied to the simultaneous dynamic differential equations of the structure. The Newmark's β step-by-step numerical integration method is applied to solve the dynamic differential equations (He et al. 2011).

3.2 Vehicle model and formulization of vehicle vibration

For the analysis of running vehicle-bridge interaction problem, a general large dump truck with one-axis at front and two-axis at rear are adopted. As shown in Figure 4, the truck is modeled as sprung-mass dynamic system with 12 DOFs, considering the dynamic motions of the vehicle body as well as the front and rear unsprung masses. The movements of the wheels are assumed compatible with the road surface. The vehicle properties and used variants are shown in Table 3 (a) and (b). Then, based on D'Alember's principle and force equilibrium on each DOF, the vehicle vibration can be formulized as follows, consider vehicle-bridge interaction.

a) Vibration equation of the vehicle body can be expressed as follows.

Sway of the body $$m_j \ddot{y}_j + \sum_{l=1}^{lx(j)} \sum_{m=1}^{2} (-1)^m v_{jylm}(t) = 0 \tag{1}$$

Bouncing of the body $$m_j \ddot{z}_j + \sum_{l=1}^{lx(j)} \sum_{m=1}^{2} v_{jzlm}(t) = 0 \tag{2}$$

Rolling of the body $$I_{jx} \ddot{\theta}_{jx} - \sum_{l=1}^{lx(j)} \sum_{m=1}^{2} (-1)^m \lambda_{jy1} v_{jzlm}(t) + \sum_{l=1}^{lx(j)} \sum_{m=1}^{2} (-1)^m \lambda_{jz1} v_{jylm}(t) = 0 \tag{3}$$

Pitching of the body $$I_{jy} \ddot{\theta}_{jy} + (-1)^l \sum_{l=1}^{lx(j)} \sum_{m=1}^{2} \lambda_{jxl} v_{jzlm}(t) = 0 \tag{4}$$

Yawing of the body $$I_{jz} \ddot{\theta}_{jz} - \sum_{l=1}^{lx(j)} \sum_{m=1}^{2} (-1)^l (-1)^m \lambda_{jxl} v_{jylm}(t) = 0 \tag{5}$$

Here, suffixes *j*, *l*, *k*, *m* and *x*, *y*, *z* are used to define the variants and parameters used in the vehicle model, and are specified as follows. *j* indicates the vehicle number. *l* = 1 or 2 denotes the front or rear suspension; *k* = 1 or 2, the front or rear wheel axle at the front or rear suspension, while in this model only *k* = 1 in the front suspension; *m* = 1 or 2, the left or right side. *x*, *y*, *z* denotes the three directions in Cartesian coordinates. $lx(j)$ is the function of vehicle number, which defines the number of suspensions in that vehicle. $v_{jlkm}(t)$ expresses the forces due to the spring deformation between the vehicle body and suspensions.

(b) Vibration equation of the suspension (unsprung mass) can be expressed as follows.

Sway of the unsprung masses $$m_{jl}\ddot{y}_{jl} - \sum_{m=1}^{2}(-1)^m v_{jylm}(t) + \sum_{k=1}^{kx(l)}\sum_{m=1}^{2}(-1)^m v_{jylkm}(t) = 0 \quad (6)$$

Parallel hop of the unsprung masses $$m_{jl}\ddot{z}_{jl} - \sum_{m=1}^{2} v_{jzlm}(t) + \sum_{k=1}^{kx(l)}\sum_{m=1}^{2} v_{jzlkm}(t) = 0 \quad (7)$$

Axle tramp of the unsprung masses

$$I_{jxl}\ddot{\theta}_{jxl} + \sum_{m=1}^{2}(-1)^m \lambda_{jz2} v_{jylm}(t) + \sum_{m=1}^{2}(-1)^m \lambda_{jy1} v_{jzlm}(t) + \sum_{k=1}^{kx(l)}\sum_{m=1}^{2}(-1)^m \lambda_{jz3} v_{jylkm}(t) - \sum_{k=1}^{kx(l)}\sum_{m=1}^{2}(-1)^m \lambda_{y2} v_{jzlkm}(t) = 0 \quad (8)$$

Windup motion of the unsprung masses $$I_{jyl}\ddot{\theta}_{jyl} + \sum_{k=1}^{kx(l)}\sum_{m=1}^{2}(-1)^k \lambda_{jx4} v_{jzlkm}(t) = 0 \quad (9)$$

where, $v_{jlkm}(t)$ expresses the forces due to the spring deformation between the vehicle body and suspensions. w_{jylkm} and w_{jzlkm} expresses the displacement at the contact point of the tire and the road surface, which is a combination of the slab deflection and the road surface roughness.

The wheel load is shown in the below equation, where g is the acceleration of gravity.

$$P_{jylkm}(t) = (-1)^m v_{jylkm}(t), \qquad P_{jzlkm}(t) = -\frac{1}{2kx(l)} g\left\{\left(1 - \frac{\lambda_{jxl}}{\lambda_{jx}}\right) m_j + m_{jl}\right\} + v_{jzlkm}(t) \quad (10)$$

Expanding and substituting the above equations, matrix form of the formulization can be derived as below, where $\boldsymbol{M}_v$, $\boldsymbol{C}_v$, $\boldsymbol{K}_v$ and $\boldsymbol{F}_v$ are mass, damping, stiffness matrixes and external force vector respectively.

$$\boldsymbol{M}_v\ddot{\boldsymbol{w}}_v + \boldsymbol{C}_v\dot{\boldsymbol{w}}_v + \boldsymbol{K}_v\boldsymbol{w}_v = \boldsymbol{F}_v \quad (11)$$

3.3 Formulization of bridge vibration

The dynamic differential equations of the bridge can be derived as follows, based on FEM theories and D'Alembert's Principle.

$$\boldsymbol{M}_b\ddot{\boldsymbol{w}}_b + \boldsymbol{C}_b\dot{\boldsymbol{w}}_b + \boldsymbol{K}_b\boldsymbol{w}_b = \boldsymbol{F}_b \quad (12)$$

where, $\boldsymbol{M}_b$, $\boldsymbol{C}_b$, $\boldsymbol{K}_b$ and $\boldsymbol{w}_b$ respectively denote the bridge mass, damping, stiffness matrices and the nodal displacement vector. Herein, the damping matrix $\boldsymbol{C}_b$ is calculated by Rayleigh damping The external force vector, $\boldsymbol{F}_b$, can be expressed as follows, where, $P_{jlk}(t)$ and $\boldsymbol{\Psi}_{jlk}(t)$ respectively denote the wheel load and the distribution vector, while h is the total vehicle number.

$$\boldsymbol{F_b} = \sum_{j=1}^{h}\sum_{l=1}^{lx(j)}\sum_{k=1}^{kx(l)} \boldsymbol{\Psi}_{jlk}(t) P_{jlk}(t) \quad (13)$$

Applying the modal analysis technique to the bridge system, the structural displacement vector, $\boldsymbol{w}_b$, can be expressed as follows using eigenvectors $\boldsymbol{\varphi}_i$ and generalized coordinates q_i, where, subscript i is the mode number and n indicates the highest one to be considered.

$$\boldsymbol{w}_b = \sum_{i=1}^{n} \boldsymbol{\varphi}_i q_i = \boldsymbol{\Phi} \cdot \boldsymbol{q} \tag{14}$$

Substitute $\boldsymbol{w}_b$ into the bridge vibration equation will obtain the following equation.

$$\boldsymbol{M}_b\boldsymbol{\Phi}\ddot{\boldsymbol{q}}+\boldsymbol{C}_b\boldsymbol{\Phi}\dot{\boldsymbol{q}}+\boldsymbol{K}_b\boldsymbol{\Phi}\boldsymbol{q}=\boldsymbol{F}_b \tag{15}$$

Multiply $\boldsymbol{\Phi}^T$ to both sides,

$$\boldsymbol{\Phi}^T\boldsymbol{M}_b\boldsymbol{\Phi}\ddot{\boldsymbol{q}}+\boldsymbol{\Phi}^T\boldsymbol{C}_b\boldsymbol{\Phi}\dot{\boldsymbol{q}}+\boldsymbol{\Phi}^T\boldsymbol{K}_b\boldsymbol{\Phi}\boldsymbol{q}=\boldsymbol{\Phi}^T\boldsymbol{F}_b \tag{16}$$

According to the orthogonality of eigenvectors, and assuming $\boldsymbol{\varphi}_i^T\ \boldsymbol{F}_b=F_i$, the bridge equation corresponding to each mode can be expressed as follows by generalized coordinates.

$$M_i\ddot{q}_i + C_i\dot{q}_i + K_i q_i = F_i \tag{17}$$

4 EIGEN VIBRATION EVALUATION

Eigenvale analyses of the the twin I-girder bridges are performed using QR method. The frequencies of the primary vertical mode (V_1) and the primary torsional mode (T_1) are respectively shown in Table 4. The parameter of frequency ratio, f_{T1}/f_{V1}, is used to evaluate the torsional stiffness. In general, this frequency ratio of a steel bridge with general open cross-section is around 2.0. As shown in Table 4, the torsional frequency of the basic model is rather low. On the other hand, the frequency ratios of the diagonal crossbeam model is 2.063, indicating that the torsional stiffness of this model is much higher than the basic model. The reason is considered as that the girders, diagonal crossbeams and the slabs form a pseudo box girder cross-section.

Table 4: Natural frequencies

Bridge model	f_{V1} (Hz)	f_{T1} (Hz)	f_{T1}/f_{V1}
Basic model	2.241	3.460	1.544
Diagonal cross-beam model	2.379	4.908	2.063

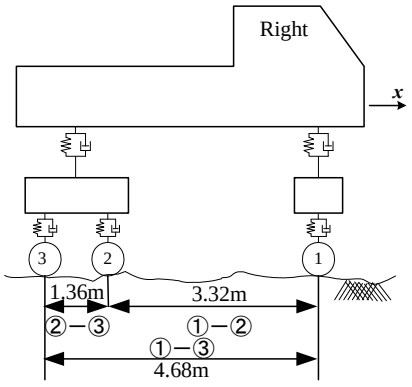

Figure 5: Distances between wheels

Table 5: Frequency of wheel excitation(Hz)

	40km/h	50km/h	60km/h
①－②	3.346	4.180	5.018
①－③	8.169	10.250	12.250
②－③	2.373	2.956	3.559

5. NUMERICAL EVALUATION ON BRIDGE VIBRATION

5.1 Analytical conditions and scenarios

The coupled vibrations of the running vehicle and the two types of bridges are simulated using the developed computer program based on the above formula to evaluate the dynamic response of the curved girder bridge. In this paper, the influence of critical vehicle running conditions, that is, the resonant excitation caused by the wheel distance and the speed of running vehicles, on the dynamic response of the bridge is elucidated. Resonant vibration will occur according to the relationship between the frequencies of primary bridge vibration modes and the excitation frequencies resulted from the wheel distances and running speed.

The wheel excitation frequency is defined as the ratio of the vehicle velocity (v) and the distance between two wheels (l), v/l. The distance between wheels are shown Figure 5, and the wheel excitation frequencies under vehicle velocities of 40km/h, 50km/h and 60km/h are given in Table 5. The wheel excitation frequencies of 40km/h (②-③, ①-②) are close to the frequencies of the primary vertical mode and the primary torsional mode of the basic bridge model. On the other hand, the wheel excitation frequency of 60km/h (②-③) is close to the frequency of the primary torsional mode of the basic model, while those of 50km/h do not have close values to the bridge frequencies.

In this analysis, the number of running vehicles is set as five, and they are running along a straight lane. The distance between vehicles is determined to ensure the drive safety in Japanese traffic rules. The output point is the center node of the main girder in longitudinal direction on the running side, whose static defection is considered to be the largest.

5.2 Dynamic response evaluation under different vehicle velocities

The vehicle velocities of 40km/h, 50km/h and 60km/h are adopted to evaluate the dynamic bridge response. In this case, only the basic bridge model is used for discussion. The acceleration and the displacement responses of the output point are respectively shown in Figure 6 and Figure 7, and their maximum values are given in Table 6. From this result, both the maximum accelaration and deflection of 40km/h are larger than those of others. The reason is considered as that the wheel excitation frequencies are close to those of the primary vertical and torsional bridge vibration modes. The second largest acceleration and deflection responses are observed in the case of 60km/h, in which the wheel excitation frequency is close to the primary torsional mode. From this result, it is clear that resonant vibration between the running vehicles and the bridge will occur according to the running conditions of the vehicles.

Table 6: Maximum acceleration and deflection of different vehicle's velocity

Vehicle speed	40km/h	50km/h	60km/h
Maximum acceleration	236.14gal	179.77gal	220.65gal
Maximam deflection	22.02mm	12.94mm	14.91mm

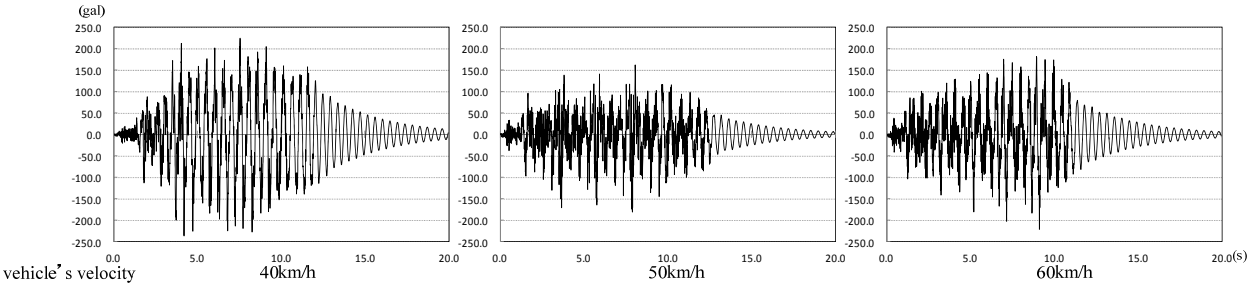

Figure 6: Acceleration responses of basic model

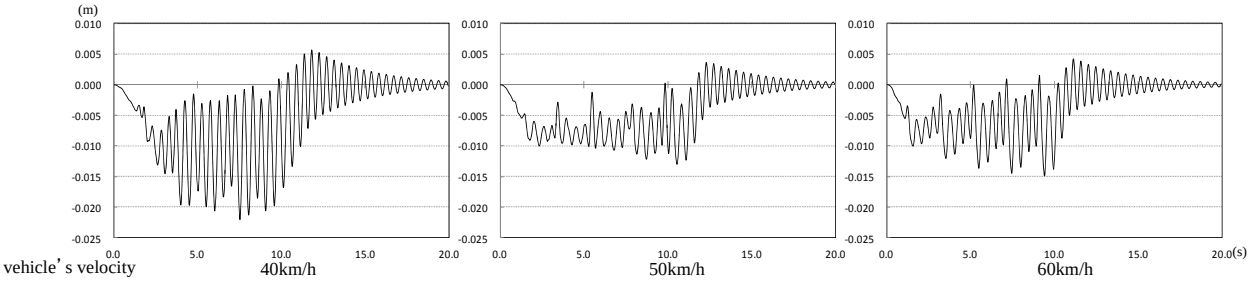

Figure 7: Displacement responses of basic model

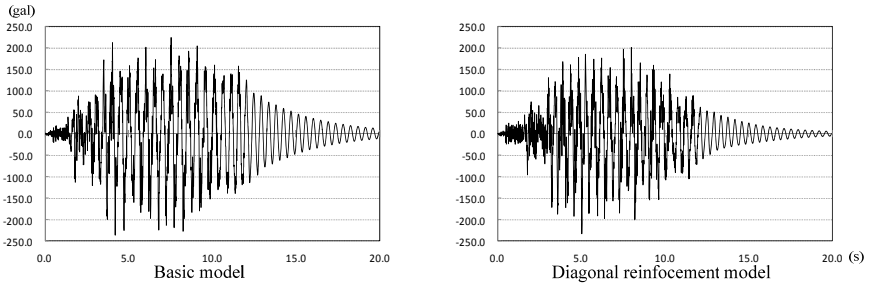

Figure 8: Acceleration and displacement responses of diagonal crossbeam model

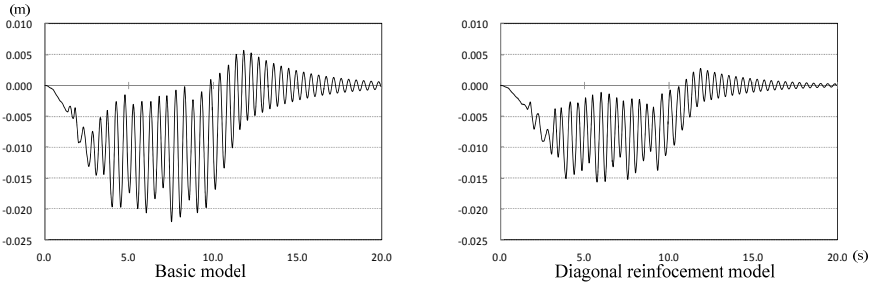

Figure 9: Acceleration and displacement responses of diagonal crossbeam model

Table 7: Maximum acceleration and deflection of different bridge model

Bridge model	Basic model	Diagonal reinforcement
Maximum acceleration	236.14gal	232.26gal
Maximum deflection	22.02mm	15.57mm

5.2 Dynamic response evaluation of different bridges

The difference of the dynamic responses of the above two types of bridges, i.e., the basic model and the diagonal crossbeam model, is also numerically evaluated in this study. Here, only the vehicle velocity of 40km/h is used. The acceleration and displacement responses of the output point are respectively shown in Figure 8 and Figure 9, and their maximum values are given in Table 8. From this result, both the maximum acceleration and deflection responses of the diagonal crossbeam model are smaller than those of the basic model. The reason is considered as that the resonance effect decreased because the primary torsional frequency of the diagonal crossbeam model is much larger than that of the basic mode.

6. CONCLUSIONS

In this paper, an analytical approach to simulate the running vehicle-bridge coupled vibration problem is formulized and coded, taking advantage of a 12-DOF general large dump truck model and a three-dimensional FE bridge model. Then, the dynamic response of the curved girder bridge are simulated and evaluate under critical vehicle running conditions, in which the influence of resonant excitation caused by the wheel distance and the speed of running vehicles on the dynamic response of the bridge is elucidated. It is clear from the numerical results that resonant vibration between the running vehicles and the bridge will occur according to the running conditions of the vehicles. Furthermore, countermeasures to increase the torsional stiffness of the bridge can influence the resonant vibration between the vehicle and bridge, which should be investigated in advance in actual engineering works. The approach established in this research is effective to discuss on the problems either of existing bridges or in the design stage of a new bridge.

REFERENCES

He X, Noda Y, Hayashikawa T, Kawatani M and Matsumoto T (2011) An analytical approach to coupled vibration of curved rationalized girder bridges and running vehicles, Proc. of The Twelfth East Asia-Pacific Conference on Structural Engineering and Construction (EASEC-12), Paper ID: 723 (CD-ROM).

Kim CW, Kawatani M, and Hwang WS (2004). Reduction of traffic-induced vibration of two-girder steel bridge seated on elastomeric bearings. Engineering Structures. 26, pp. 2185-2195.

Linzell DG., Hall D and White D (2004). Historical perspective on horizontally curved I girder bridge design in the United States, Journal of Bridge Engineering, 9(3), pp. 218-229.

Yoon KY, Kang YJ, Choi YJ, and Park NH (2005). Free vibration analysis of horizontally curved steel I-girder bridges. Thin-Walled Structures. 43, pp. 679-699.